Pressure Transient Analysis Considering Geo-mechanic Effects in Deep Oil Reservoirs

Maolin Xu, Dongyan Fan, and Jun Yao

Abstract Considering the characteristics of high pressure and high stratum stress in deep reservoirs and in order to study the interaction between seepage field and stress field in the development of deep reservoirs, pressure transient analysis models of three different well types are established considering geo-mechanic effects for deep oil reservoirs, including vertical wells, horizontal wells, and fractured horizontal wells. The models are solved by finite element method and pressure responses are analyzed and compared with or without geo-mechanic effects. The result shows that both the pressure and pressure derivative curves are upward when considering stress field, where porosity and permeability decrease due to the deformation in deep reservoir, and the degree of permeability reduction is greater than that of porosity. And well testing curves are upward more obviously if the value of rocks resisting deformation is smaller. Finally, the parameters of fracture width, fracture length, and distance between fractures in multi-staged fractured horizontal wells are discussed.

Keywords Deep oil reservoir · Well testing analysis · Fluid solid coupling · Finite element method

1 Introduction

Deep oil reservoirs refer to oil reservoirs with burial depths ranging from 3500 to 4500 m or more. With the continuous development of mid or shallow oil and gas, its potential for development is becoming smaller and smaller. The development of deep and ultra-deep reservoirs has become an inevitable trend. Most deep oil and gas reservoirs are low porosity and low permeability reservoirs. If artificial stimulation is not used and only natural production capacity is relied on, the production rate is very low. Therefore, horizontal wells and fractured horizontal wells are the main ways to improve production capacity [1]. Under high-stress conditions, as development progresses, the reservoir pressure gradually decreases, and changes in fluid

M. Xu (✉) · D. Fan · J. Yao
School of Petroleum Engineering, China University of Petroleum, Qingdao 266580, China
e-mail: S18020143@s.upc.edu.cn

S. Li (ed.), *Computational and Experimental Simulations in Engineering*, Mechanisms and Machine Science 146, https://doi.org/10.1007/978-3-031-44947-5_100

pressure can cause changes in the effective stress of the rock, leading to the deformation of the rock skeleton. At the same time, the deformation of the rock skeleton will, in turn, affect the reservoir physical properties (porosity and permeability) of the rock, thereby affecting the seepage process. This is the problem of fluid–solid coupling. Therefore, it is necessary to establish a fluid–solid coupling seepage theory to accurately describe and simulate the seepage process in deep oil reservoirs [2].

Terzaghi was the first to study the interaction between rocks and fluids and proposed the famous effective stress formula [3]. Biot established the Biot consolidation theory, laying the foundation for the study of underground fluid–solid coupling [4, 5]. Dong Pingchuan and others extended the Biot theory to the case of multiphase fluid and rock elastoplasticity [6]. Ran Qiquan and others studied the theory and method of fluid–solid coupling using the reservoir numerical simulation method considering fluid changes under stress changes [7]. Dr. Zhou Zhijun introduced the fluid solid coupling theory in low-permeability reservoirs and analyzed the impact of stress on the development and production of low-permeability reservoirs [8]. Chin et al., Pinzon et al., Tao et al. combined seepage mechanics with solid mechanics to establish a fluid solid coupling seepage model and study its impact on well testing, but it was not widely used [9–11]. Samanigeo established a well testing model that only considers stress sensitivity [12]. Pedrosa and Kikani et al. [13, 14] first introduced permeability modulus, expressed as an exponential form of pore fluid pressure, and studied the impact of different permeability moduli on well testing. Zhang Zhang analyzed the pressure recovery well testing analysis considering the influence of medium deformation on reservoir physical properties [15]. Therefore, this article establishes the model based on fluid–solid coupling of seepage field and stress field, and studies the well testing problem of deep oil reservoirs under high stress conditions.

2 Establishment of Model

2.1 Physical Parameters

Vertical well. A vertical well is in the center of a closed (or constant pressure) boundary reservoir. The reservoir and vertical well parameters are: original formation pressure $p_i = 60$ MPa, reservoir radius $R_e = 3000$ m, oil well radius $R_w = 0.1$ m, initial permeability $k_0 = 10^{-3}$ μm^2, initial porosity $\phi_0 = 0.1$. The fluid viscosity is 2 mPa s, and the fluid density is 900 kg/m^3. The density of the reservoir rock is 2500 kg/m^3, the elastic modulus E is 2000 MPa, and the Poisson's ratio ν is 0.25. Assumptions are followed: fixed production; Rock is a porous medium and the rock skeleton has elastic deformation; The porous medium is full of single-phase fluid, and the fluid is slightly compressibility; Fluid flow conforms to Darcy's law; Neglecting the effects of capillary force, and gravity; circular homogeneous reservoir.

Horizontal well. A horizontal well is in the center of closed (or constant pressure) boundary reservoir. The length of the horizontal well is 500 m, and other parameters are the same as those of the vertical well.

Fractured horizontal wells. A horizontal well with three equally spaced segmented fractures is located in the center of the closed (or constant pressure) boundary reservoir. The horizontal well is 1000 m long, the fracture width is 0.3 mm, the fracture length is 100 m, and the distance between fractures is 500 m. The other parameters are the same as vertical wells.

2.2 Mathematical Model

Seepage field. As shown in Eq. (1), due to the deformation of the rock skeleton, the absolute velocity of the fluid is equal to the sum of the absolute velocity of the solid phase particles of the rock and the relative velocity of the fluid relative to the solid phase particles of the rock.

$$v_{\mathrm{o}} = v_{\mathrm{s}} + v_{\mathrm{os}} \tag{1}$$

where v_{o} is the absolute velocity of the fluid, v_{s} is the absolute velocity of solid particles in rocks, v_{os} is the relative velocity of the fluid relative to the solid phase particles of rocks. The relative velocity of the fluid relative to the solid phase particles of rocks is called the seepage velocity, which is $v_{\mathrm{os}} = v$. Derived from Darcy's law

$$v = -\frac{k}{\mu}\nabla(\overline{p} - \gamma_{\mathrm{w}} D) \tag{2}$$

where $\overline{p}$ is the fluid pressure, γ_{w} is the weight of formation water, D is depth. Derive the formula

$$v_{\mathrm{o}} = v_{\mathrm{s}} - \frac{k}{\mu}\nabla(\overline{p} - \gamma_{\mathrm{w}} D) \tag{3}$$

Equation (4) obtained from the Continuity equation

$$\mathrm{div}(\rho \overline{\boldsymbol{v}}) + \frac{\partial(\rho\phi)}{\partial t} = 0 \tag{4}$$

Substitute Eq. (3) into Eq. (4) and we can yield the seepage equation (5) with a stress field phase, $\overline{\boldsymbol{v_s}}$ is a coupled phase that need to be solved by connecting the stress field.

$$\mathrm{div}\left[\rho\left[\overline{\boldsymbol{v_{\mathrm{s}}}} - \frac{k}{\mu}\nabla(\overline{p} - \gamma_{\mathrm{w}} D)\right]\right] + \frac{\partial(\rho\phi)}{\partial t} = 0 \tag{5}$$

where

$$\overline{\boldsymbol{v}_{\mathrm{s}}} = \left(\frac{\partial u}{\partial t}, \frac{\partial v}{\partial t}, \frac{\partial w}{\partial t} \right)$$
$$\mathbf{U} = \left(u \ v \ w \right)$$

$\overline{\boldsymbol{v}_{\mathrm{s}}}$ is the velocity vector of solid particles in rocks, $\mathbf{U}$ is the displacement vector of rock particles.

Deep oil reservoirs are in a high-stress state, and with oil and gas production, the reservoir pressure decreases, causing stress changes, and the direct result is the deformation of the reservoir medium. At this time, porosity and permeability will inevitably change. Relevant scholars have conducted extensive research on how to express porosity and permeability. This article cites the research results of Ran et al. [16], starting from the reservoir medium, porosity and permeability can be expressed as the relationship between initial values and rock deformation, as shown in Eqs. (6) and (7)

$$\varnothing = \frac{\phi_0 + \varepsilon_{\mathrm{v}}}{1 + \varepsilon_{\mathrm{v}}} \tag{6}$$

$$k = \frac{\left(1 + \frac{\varepsilon_{\mathrm{v}}}{\phi_0}\right)^3}{1 + \varepsilon_{\mathrm{v}}} k_0 \tag{7}$$

where ϕ_0 is the initial porosity, k_0 is the initial permeability, ε_{v} is volume strain of rock skeleton $\varepsilon_{\mathrm{v}} = \varepsilon_{\mathrm{x}} + \varepsilon_{\mathrm{y}} + \varepsilon_{\mathrm{z}}$.

Stress field. Assuming a homogeneous and isotropic geotechnical element *dxdydz* as shown in Fig. 1, the stress state at a point can be represented by nine stress components on three adjacent surfaces σ_{x}, τ_{xy}, τ_{xz}, τ_{yx}, σ_{y}, τ_{yz}, τ_{zx}, τ_{zy}, σ_{z} [17]. By equilibrium conditions $\sum F_{\mathrm{y}} = 0 \sum F_{\mathrm{z}} = 0 \sum F_{\mathrm{x}} = 0$. The equilibrium conditions that need to be met when the object is in equilibrium are shown in Eq. (8)

$$\begin{cases} \frac{\partial \sigma_{\mathrm{x}}}{\partial x} + \frac{\partial \tau_{\mathrm{yx}}}{\partial y} + \frac{\partial \tau_{\mathrm{zx}}}{\partial z} + f_{\mathrm{x}} = 0 \\ \frac{\partial \tau_{\mathrm{xy}}}{\partial x} + \frac{\partial \sigma_{\mathrm{y}}}{\partial y} + \frac{\partial \tau_{\mathrm{zy}}}{\partial z} + f_{\mathrm{y}} = 0 \\ \frac{\partial \tau_{\mathrm{xz}}}{\partial x} + \frac{\partial \tau_{\mathrm{yz}}}{\partial y} + \frac{\partial \sigma_{\mathrm{z}}}{\partial z} + f_{\mathrm{z}} = 0 \end{cases} \tag{8}$$

where f_{x}, f_{y}, f_{z} is the volume force.

A 3×3 matrix $\varepsilon_{\mathrm{ij}}$ is used for the strain at a point in the reservoir rock. In the spatial problem of reservoir rock deformation, the relationship between strain components and displacement components is described by the geometric equation as Eq. (9)

$$\varepsilon_{\mathrm{ij}} = \begin{bmatrix} \varepsilon_{\mathrm{x}} & \frac{1}{2}\gamma_{\mathrm{yx}} & \frac{1}{2}\gamma_{\mathrm{zx}} \\ \frac{1}{2}\gamma_{\mathrm{xy}} & \varepsilon_{\mathrm{y}} & \frac{1}{2}\gamma_{\mathrm{zy}} \\ \frac{1}{2}\gamma_{\mathrm{xz}} & \frac{1}{2}\gamma_{\mathrm{yz}} & \varepsilon_{\mathrm{z}} \end{bmatrix}$$

Fig. 1 Stress state of a point

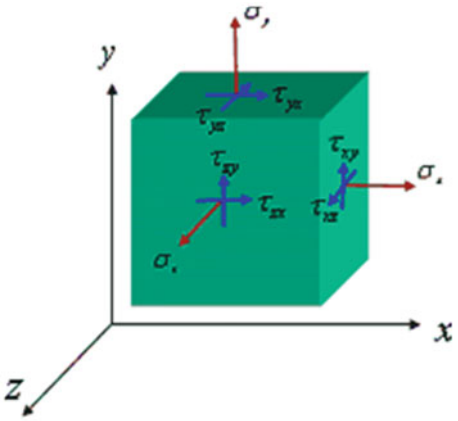

$$\times \begin{cases} \varepsilon_x = \frac{\partial u}{\partial x} \quad \varepsilon_y = \frac{\partial v}{\partial y} \quad \varepsilon_z = \frac{\partial w}{\partial z} \\ \gamma_{yz} = \frac{\partial w}{\partial y} + \frac{\partial v}{\partial z} \\ \gamma_{xz} = \frac{\partial u}{\partial z} + \frac{\partial w}{\partial x} \\ \gamma_{xy} = \frac{\partial v}{\partial x} + \frac{\partial u}{\partial y} \end{cases} \tag{9}$$

Fluid solid coupling. When the reservoir rock is in an elastic deformation state, the stress and strain follow the generalized Hooke's law [18], which can be represented by Eq. (10) as

$$\begin{cases} \sigma_x = \lambda\varepsilon_v + 2G\varepsilon_x \\ \sigma_y = \lambda\varepsilon_v + 2G\varepsilon_y \\ \sigma_z = \lambda\varepsilon_v + 2G\varepsilon_z \\ \tau_{yz} = G\gamma_{yz} \\ \tau_{xz} = G\gamma_{xz} \\ \tau_{xy} = G\gamma_{xy} \end{cases} \tag{10}$$

where $\lambda = \frac{E\nu}{(1+\nu)(1-2\nu)}$, $G = \frac{E}{2(1+\nu)}$, E is the Elastic modulus, ν is Poisson's ratio, G is shear modulus, λ is the Lamé constant. Or the stress–strain relationship can be expressed by an elastic matrix.

$$\sigma_{ij} = [D]_e \varepsilon_{ij} \tag{11}$$

where $[D]_e$ is an elastic matrix, whose specific expression is

$$[D]_{\mathrm{e}} = \frac{E}{1+\nu}\begin{bmatrix} \frac{1-\nu}{1-2\nu} & \frac{\nu}{1-2\nu} & \frac{\nu}{1-2\nu} & 0 & 0 & 0 \\ \frac{\nu}{1-2\nu} & \frac{1-\nu}{1-2\nu} & \frac{\nu}{1-2\nu} & 0 & 0 & 0 \\ \frac{\nu}{1-2\nu} & \frac{\nu}{1-2\nu} & \frac{1-\nu}{1-2\nu} & 0 & 0 & 0 \\ 0 & 0 & 0 & \frac{1}{2} & 0 & 0 \\ 0 & 0 & 0 & 0 & \frac{1}{2} & 0 \\ 0 & 0 & 0 & 0 & 0 & \frac{1}{2} \end{bmatrix}$$

Terzaghi believes that rock deformation is controlled by the effective stress of the rock, and the total stress experienced by the formation rock is the pressure of the overlying rock layer. The effective stress is the pressure of the overlying rock layer minus the pore fluid pressure, and the effective stress formula is given

$$\sigma_{\mathrm{ij}} = \sigma'_{\mathrm{ij}} + \delta_{\mathrm{ij}}\overline{p} \tag{12}$$

where σ_{ij} is the total stress, σ'_{ij} is the effective stress, $\overline{p}$ is the pore fluid pressure, δ_{ij} is the Kronecker function. The effective stress ultimately determines the deformation of the rock. According to the principle of effective stress, ignoring the influence of gravity, Eq. (12) is substituted into Eq. (8) to obtain the following Eq. (13)

$$\begin{cases} \frac{\partial \sigma'_{\mathrm{x}}}{\partial x} + \frac{\partial \tau_{\mathrm{yx}}}{\partial y} + \frac{\partial \tau_{\mathrm{zx}}}{\partial z} + \frac{\partial \overline{p}}{\partial x} = 0 \\ \frac{\partial \tau_{\mathrm{xy}}}{\partial x} + \frac{\partial \sigma'_{\mathrm{y}}}{\partial y} + \frac{\partial \tau_{\mathrm{zy}}}{\partial z} + \frac{\partial \overline{p}}{\partial y} = 0 \\ \frac{\partial \tau_{\mathrm{xz}}}{\partial x} + \frac{\partial \tau_{\mathrm{yz}}}{\partial y} + \frac{\partial \sigma'_{\mathrm{z}}}{\partial z} + \frac{\partial \overline{p}}{\partial z} = 0 \end{cases} \tag{13}$$

We combine Eqs. (9) and (10) to obtain the Biot consolidation differential Eq. (14) represented by displacement. The pressure term is a coupling term and needs to be linked to the seepage equation to solve.

$$\begin{cases} G\nabla^2 U + (\lambda + G)\left[\frac{\partial(\nabla U)}{\partial x}\right] + \frac{\partial \overline{p}}{\partial x} = 0 \\ G\nabla^2 U + (\lambda + G)\left[\frac{\partial(\nabla U)}{\partial y}\right] + \frac{\partial \overline{p}}{\partial y} = 0 \\ G\nabla^2 U + (\lambda + G)\left[\frac{\partial(\nabla U)}{\partial z}\right] + \frac{\partial \overline{p}}{\partial z} = 0 \end{cases} \tag{14}$$

Equations (5) and (14) together form the coupled equation of seepage and stress fields.

2.3 Definite Solution Conditions

Definite solution conditions for seepage field. *Outer boundary conditions.* (1) The constant pressure outer boundary condition is a given outer boundary pressure, and its expression is

$$\mathrm{p}(r_\mathrm{e}, t) = p_\mathrm{i} \quad t > 0 \tag{15}$$

where r_e is the drainage radius, p_i is the original reservoir pressure. (2) The closed outer boundary, which is a boundary condition with no fluid flow, is expressed as

$$\frac{\partial P}{\partial r}|_{r=r_\mathrm{e}} = 0 \tag{16}$$

Internal boundary condition (1) Determine well production rate

$$\mathrm{r}\frac{\partial P(r,t)}{\partial r}|_{r_\mathrm{w}} = const \quad t > 0 \tag{17}$$

(2) Fixed bottom hole pressure

$$\mathrm{P}(r_\mathrm{w}, \mathrm{t}) = p_\mathrm{wf} = const \quad t > 0 \tag{18}$$

where r_w is the diameter of the well, p_wf is the bottom hole flow pressure.

Initial conditions. The initial condition is the distribution of reservoir pressure at the initial time, which can be expressed as

$$\mathrm{p}(\mathrm{r}, 0) = p_\mathrm{i} \quad r_\mathrm{w} < r < r_\mathrm{e} \tag{19}$$

Conditions for determining the stress field. The conditions for determining the solution of the stress field include stress boundary conditions and displacement boundary conditions.

$$F_\mathrm{Bi} = \sigma_\mathrm{ij} l_\mathrm{i} \tag{20}$$

where l is the Direction cosine.

$$U_\mathrm{Bi} = U_\mathrm{i} \tag{21}$$

2.4 Model Solving

This article establishes physical models for vertical wells, horizontal wells, and multi-staged fractured horizontal wells in deep oil reservoirs. The model is simplified to a two-dimensional plane model and solved using the finite element method to simplify the calculation.

3 Analysis of Calculation Results

3.1 Vertical Well

Typical curve analysis. Figure 2 shows that the pressure and pressure derivative curves are upward after the coupling of the stress field. This is because after considering stress coupling, the reservoir medium will undergo deformation, decreasing porosity and permeability. A more considerable pressure difference is required to maintain the same production rate, resulting in an upward trend in pressure and pressure derivative curves. This difference will become greater with the development and production of oil reservoirs.

Figure 3 shows the well test curves with changed boundary conditions, and due to the influence of the closed boundary, the pressure derivative tilts upwards. However, the curve is the same as the constant pressure boundary before the boundary effect.

Changes of porosity and permeability. In order to study the deformation of reservoir media, a two-dimensional cross-section is taken in the model, starting from the wellbore and ending at the reservoir boundary. Several time points of 10^5 s, 10^6 s, 10^7 s, 10^8 s and 10^9 s were taken to plot the strain variation with distance from the well, as shown in Fig. 4.

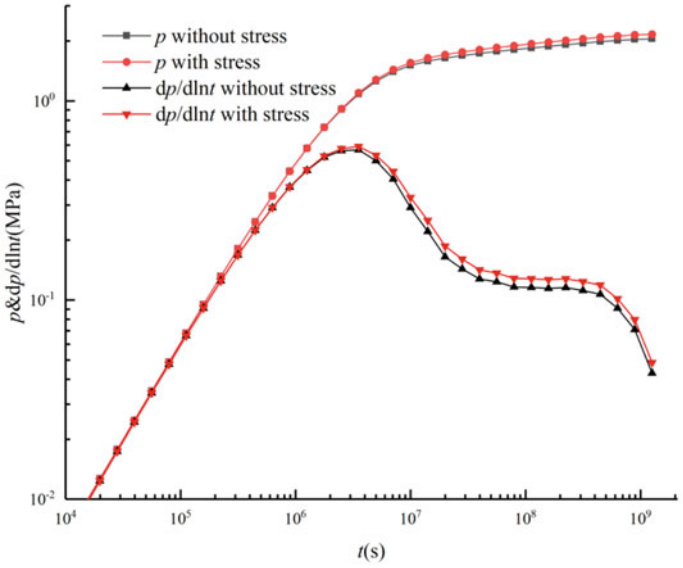

Fig. 2 Vertical well testing curve (constant pressure boundary)

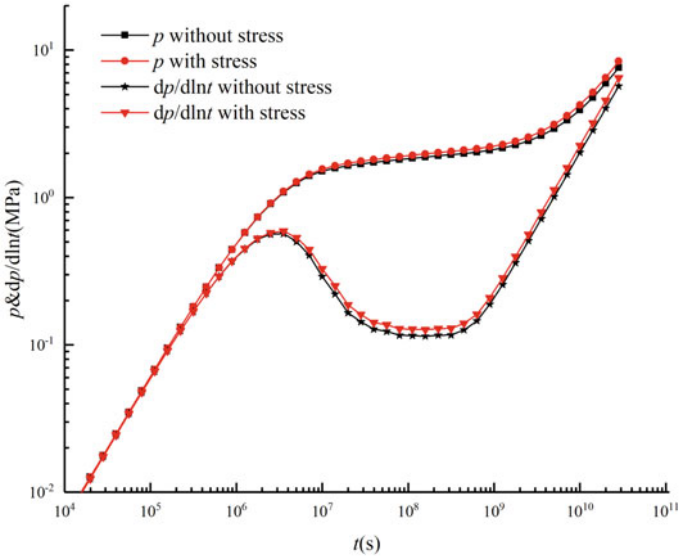

Fig. 3 Vertical well testing curve (closed boundary)

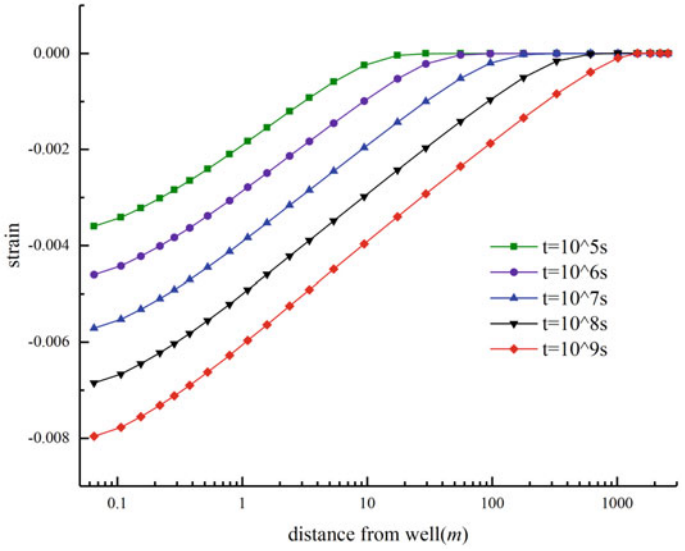

Fig. 4 Strain change curve

With the development of the reservoir, the fluid pressure in the reservoir decreases, while the pressure of the overlying rock layer remains unchanged. The effective stress on the reservoir rock will increase. The rock will be compressed, the volume will decrease, and the strain will be negative. From Fig. 4, it can be seen that the strain mainly occurs near the bottom of the well, with a maximum of − 0.008. At 10^5 s, due to the short distance of pressure wave propagation, there is only deformation of reservoir rock near the well. With the development and production of oil reservoirs, pressure spreads to the remote well zone, and rock deformation also begins to occur in the remote well zone. At 10^9 s, there is a strain in the far well area.

The physical properties of reservoir rocks are closely related to the deformation of the medium, as shown in Figs. 5 and 6, which show the changes in porosity and permeability within the reservoir range. From Figs. 5 and 6, the porosity and permeability change mainly occur near the bottom of the well at the early stage. In the later stage of seepage, the porosity and permeability in the far well zone also begin to decrease. Moreover, at the same time and distance from the well, the change in porosity is smaller than the change in permeability. For example, at the time of 10^9 s and the distance of 100 m from the well, the porosity has changed by 2%, while the permeability has changed by about 6%. Therefore, in some scholars' research on fluid–solid coupling in reservoirs, porosity changes should be ignored.

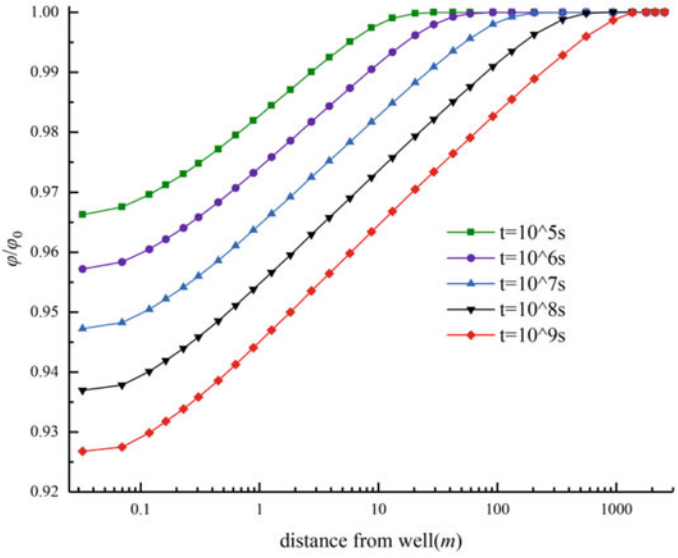

Fig. 5 Porosity change curve

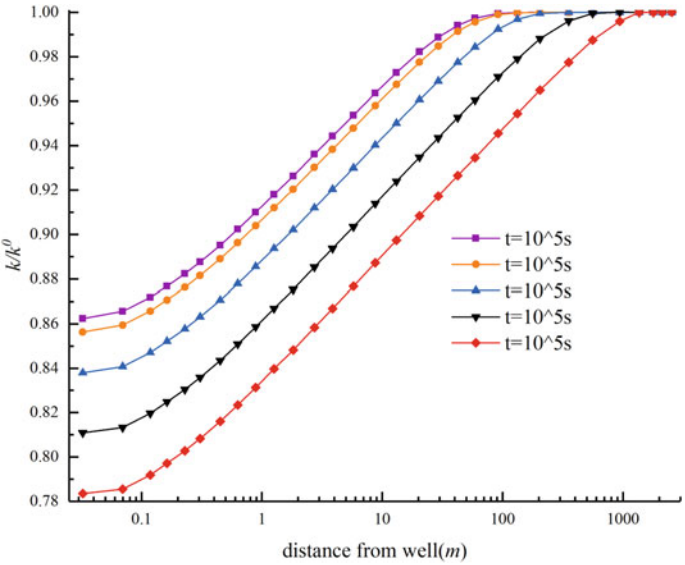

Fig. 6 Permeability change curve

3.2 Horizontal Well

A horizontal well model was established. The seepage flow in a horizontal well reservoir can be divided into three stages: early linear flow stage, middle radial flow stage, and later stage of boundary influence. The schematic diagrams of linear and radial flow in horizontal wells are shown in Fig. 7.

The stress was coupled into a horizontal well, and the fluid–solid coupling horizontal well testing curves were obtained, as shown in Figs. 8 and 9. From Figs. 8 and 9, it can be seen that, like vertical wells, under the coupling of stress fields, both the pressure and pressure derivatives exhibit an upward warping phenomenon.

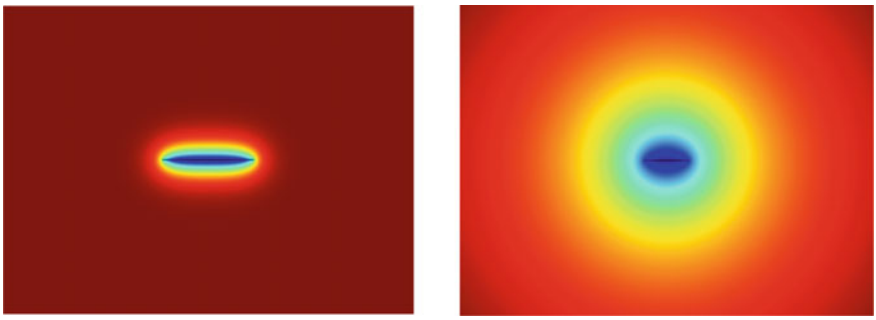

Fig. 7 Schematic diagram of linear and radial flow in horizontal wells

Moreover, the pressure and pressure derivative difference is more significant in the later stage of seepage.

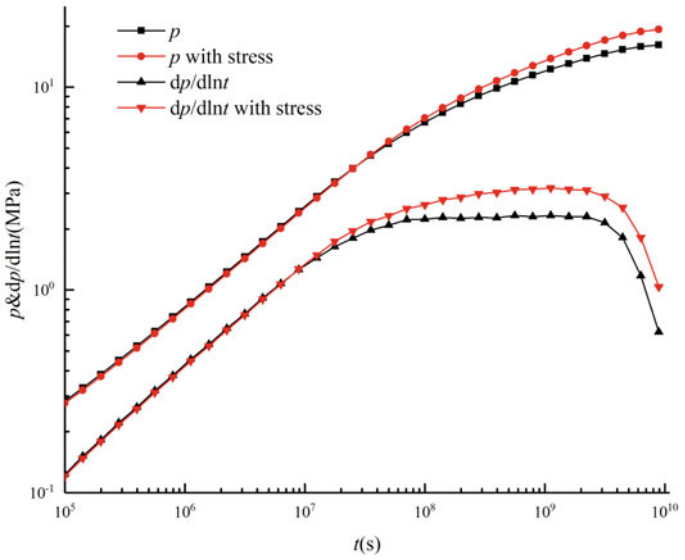

Fig. 8 Horizontal well testing curve (constant pressure boundary)

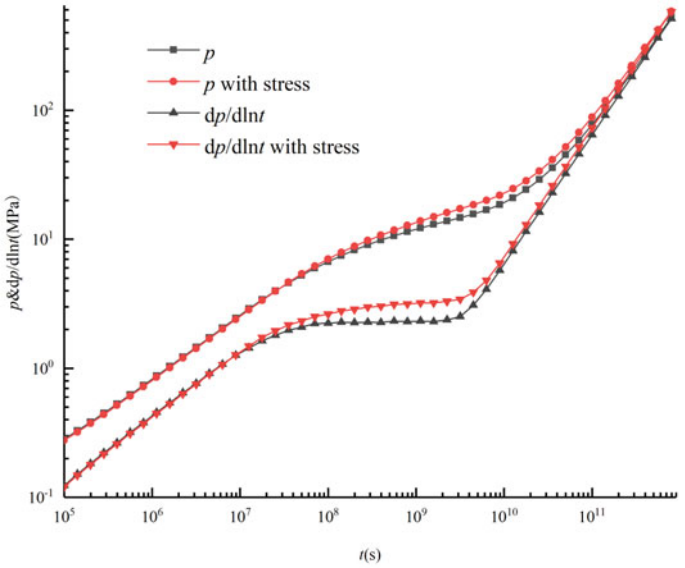

Fig. 9 Horizontal well testing curve (closed boundary)

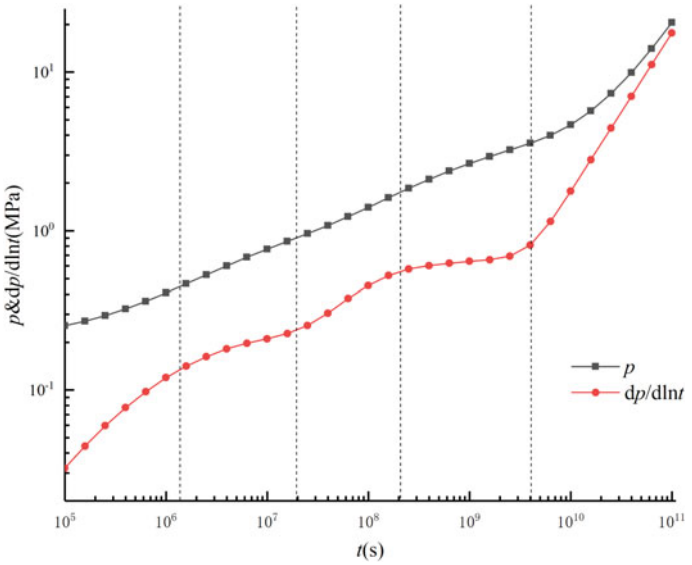

Fig. 10 Typical curve of closed boundary for fractured horizontal wells

3.3 Fractured Horizontal Wells

Typical curve analysis. Firstly, the situation without considering stress coupling was simulated. The double logarithmic coordinates were taken to obtain the pressure and pressure derivative curves (closed boundary) of the horizontal fracturing well, as shown in Fig. 10.

Figure 10 shows that multi-staged fractured horizontal wells can be divided into five flow states: I early fracture linear flow stage (first linear flow), II early fracture radial flow stage (first radial flow), III formation linear flow stage (second linear flow), IV formation radial flow stage (second radial flow), V closed boundary effect, and the double logarithmic curve shows pressure derivative curve tilting up and overlapping with the pressure curve (Fig. 11).

The stress is coupled to the multi-staged fractured horizontal well, and the well testing curves are obtained, as shown in Figs. 12 and 13. Similarly, after coupling with a stress field, the pressure and pressure derivative curves are upward. Even in the early fracture radial flow stage, the horizontal section of the pressure derivative becomes less noticeable. The well-testing curve is usually complex and variable in actual oilfield well testing, and abnormal phenomena often occur. We need to learn to analyze the reasons for them.

Stress parameter analysis. The influence of stress parameters on the well-testing curves of fractured horizontal wells is studied. Assuming a constant pressure boundary, calculations are carried out with Elastic modulus E = 3000 MPa, E =

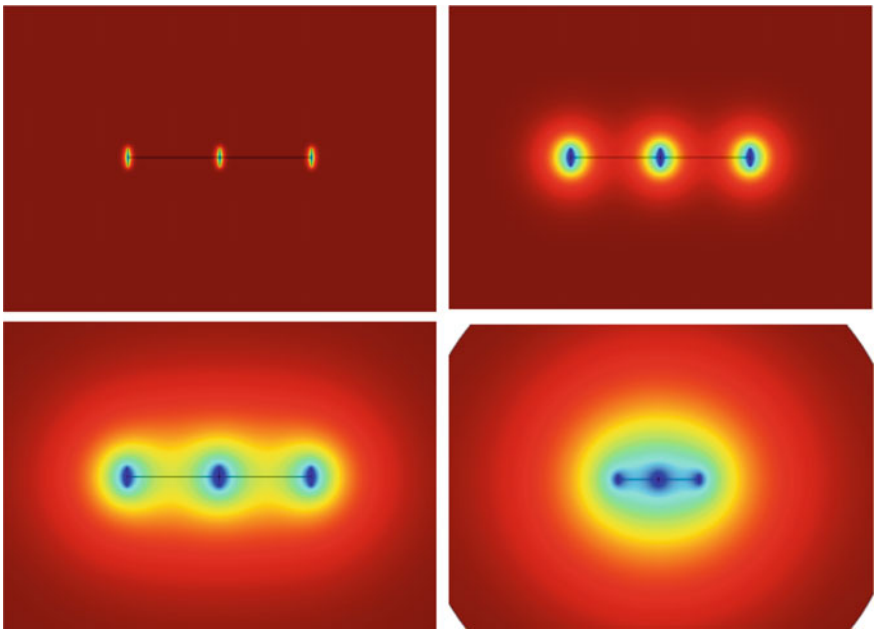

Fig. 11 Flow stages I–IV in multi-staged fractured horizontal wells

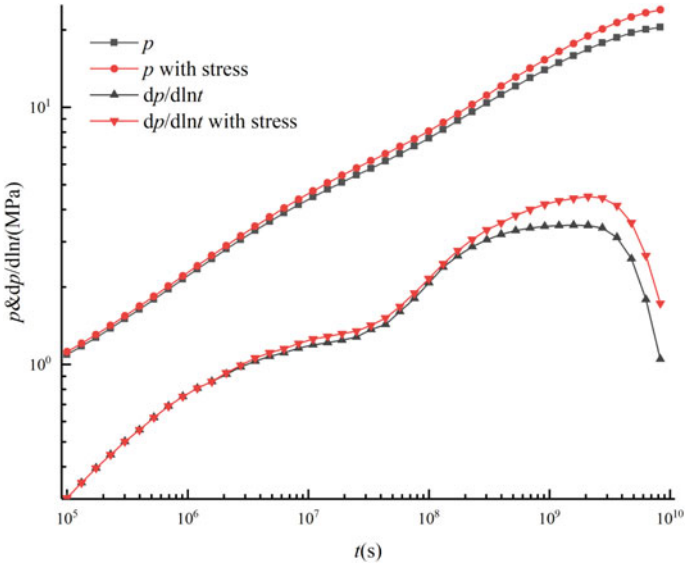

Fig. 12 Well testing curve of fractured horizontal well (constant pressure boundary)

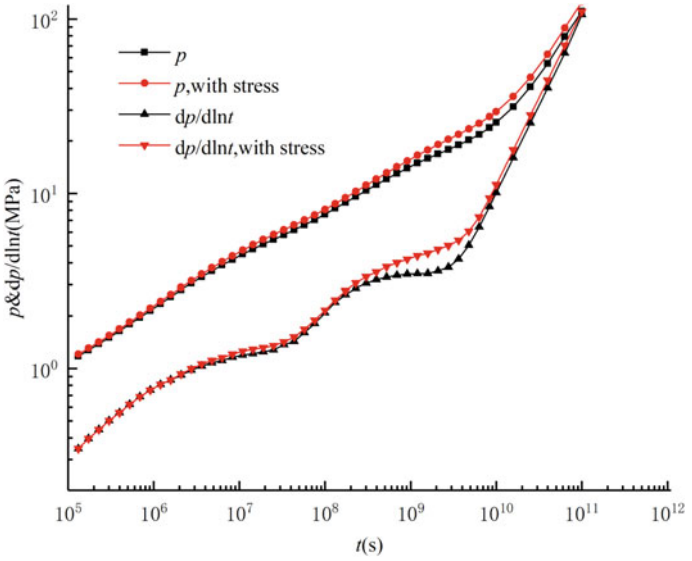

Fig. 13 Well testing curve of fractured horizontal well (closed boundary)

6000 MPa, and without considering stress coupling. Moreover, Poisson's ratio $\upsilon = 0.25$, $\upsilon = 0.35$ and without considering stress coupling. The calculation results are shown in Figs. 14 and 15.

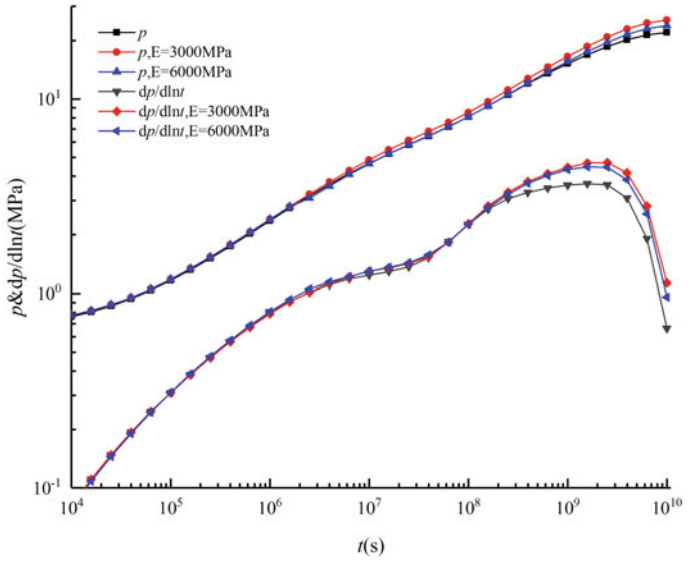

Fig. 14 Elastic modulus sensitivity analysis

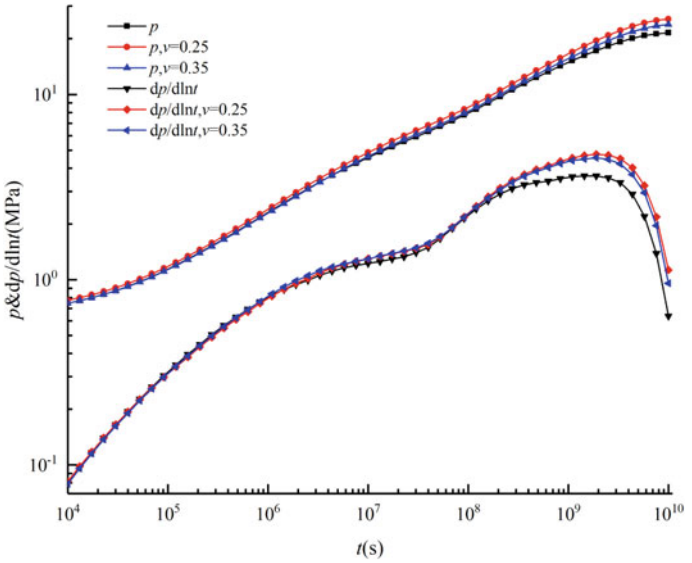

Fig. 15 Poisson's ratio sensitivity analysis

Elastic modulus is a measure of the ability of an object to resist elastic deformation. The smaller the value Elastic modulus is, the smaller the rock's ability to resist deformation. The corresponding pressure and pressure derivative curves are more pronounced as they rise upwards. At this point, stress coupling will significantly impact the well-testing curve, especially for rocks with smaller elastic moduli, such as sandstone and limestone. The factors affecting it cannot be ignored. Poisson's ratio is defined as the ratio of the transverse deformation to the longitudinal deformation of a material when subjected to tensile or compressive forces. Figure 15 shows that with the smaller value of Poisson's ratio, the corresponding pressure and pressure derivative curves are more pronounced as they rise upwards. Moreover, the stress sensitive phenomenon has a relatively small impact on the early flow stage of the well testing curve, mainly affecting the formation radial flow and boundary reflection stage. This is because the initial pressure reduction is not significant. The stress field has little effect on the seepage field. From Figs. 14 and 15, as the resistance of reservoir rocks to deformation decreases, the radial flow stage will become increasingly unclear.

Fracture parameter analysis. In order to study the influence of fracture parameters on the well testing curves of multi-staged fractured horizontal wells, different parameter values of fracture width, fracture length, and distance between fractures are taken for simulation calculation, and the influence of these parameters on the well testing curve and seepage process is analyzed.

Fracture width. Calculate with fracture widths of 0.3, 0.2, and 0.1 mm, as shown in Fig. 16.

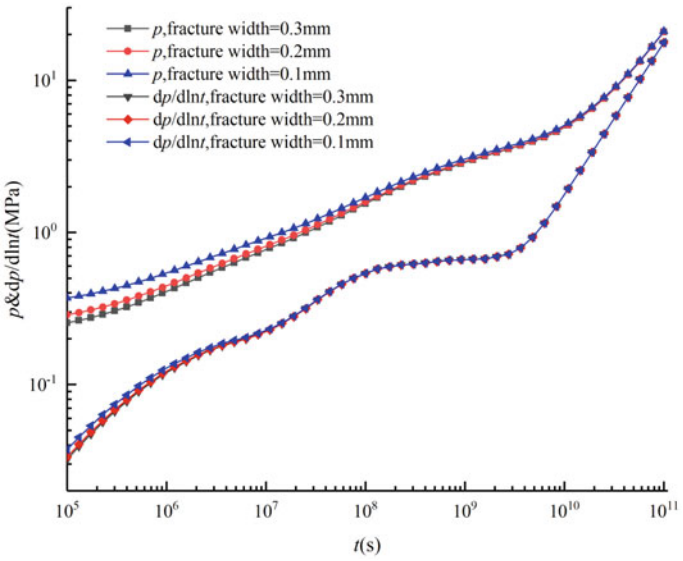

Fig. 16 Sensitivity analysis of fracture width

Figure 16 shows that the influence of fracture width on the well testing curve is mainly reflected in the early and middle stages and has almost no effect on the later stage of seepage. The wider the fracture, the smaller the value of corresponding pressure and pressure derivative, reflected in the fracture linear flow stage, fracture radial flow stage, and formation linear flow stage of seepage. This is because the wider the fracture, the stronger the conductivity of the medium and the smaller the seepage resistance. The required pressure difference will be reduced to maintain the same production speed. The main factor affecting seepage for the formation radial flow stage in the middle and later stages are matrix permeability. The role played by fracture width is relatively small and can be ignored.

Fracture length. Calculate with fracture length of 100, 150 and 200 m, as shown in Fig. 17.

Figure 17 shows that the influence of fracture length on the well testing curves is mainly reflected in the early and middle stages and has almost no effect on the later stage of seepage. The longer the fracture, the lower the corresponding pressure and pressure derivative curves, which are reflected in the fracture linear and radial flow stages. This is because the longer the fracture, the stronger the conductivity, and the smaller the seepage resistance is. The required pressure difference will be reduced to maintain the same production speed. For the formation radial flow stage in the middle and later stages, the role of fractures is relatively small, and the curves tend to overlap. From Fig. 17, it can also be seen that the longer the fracture, the less obvious the horizontal section of the pressure derivative curve is in fracture radial flow stage.

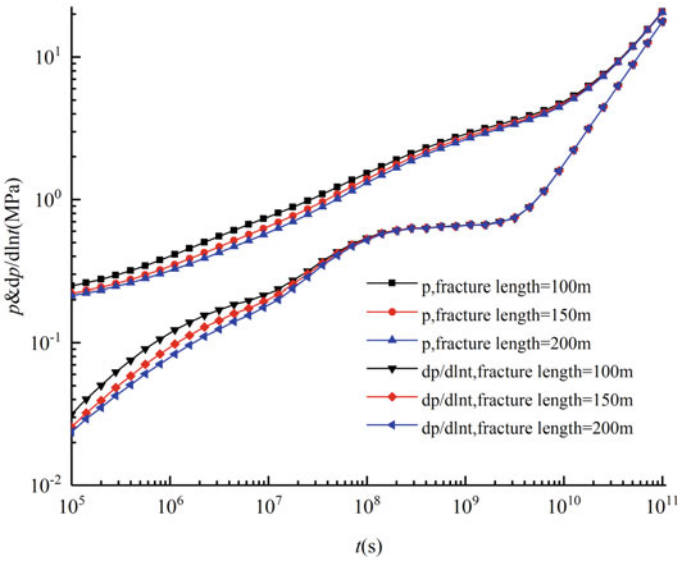

Fig. 17 Sensitivity analysis of fracture length

This is because the longer the fracture, the more difficult it is to transition from linear flow to radial flow, and the pressure wave at this time tends to be elliptical.

Fracture distance. Calculate with distance between fractures of 300, 400, and 500 m, as shown in Fig. 18.

Figure 18 shows that the distance between fractures mainly affects the fracture radial flow stage and the formation linear flow stage. In contrast, the distance between fractures unaffected the early fracture linear flow stage. The closer the distance between fractures, the less noticeable the fracture radial flow stage, and the earlier it enters the formation linear flow stage. This is because the closer the distance between fractures, the earlier the interference between fractures occurs, so the horizontal section of the pressure derivative curves is not easy to appear. However, it does not affect the formation radial flow stage and boundary effects stage.

4 Conclusions

1. The well-testing curves considering stress field coupling have higher pressure and pressure derivative curves than those without stress field coupling. Moreover, the more noticeable this coupling effect is in the later stage of seepage.
2. After considering geo-mechanic effects, negative strain occurs in the medium within the reservoir range, resulting in a decrease of porosity and permeability in the reservoir medium. However, the decrease in porosity is much less than that of

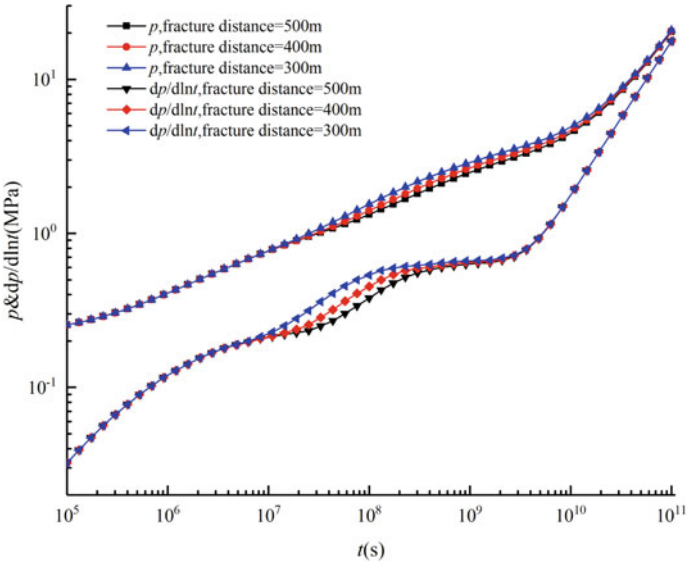

Fig. 18 Sensitivity analysis of fracture spacing

permeability. In the early stage of seepage, this effect only occurred in the near wellbore zone. As the seepage progresses, the coupling effect gradually extends to the far wellbore zone. However, the coupling effect in the near wellbore zone is still significant, while the coupling effect in the far wellbore zone is relatively small.

3. The stress parameters Elastic modulus and Poisson's ratio influence the upward amplitude of pressure and pressure derivatives. The stronger the rock's ability to resist deformation, the less noticeable the degree of change of well-testing curves.
4. (1) The width of fractures mainly affects the early and middle stages of the well testing curves of multi-staged fractured horizontal wells. The wider the fracture. The smaller the degree of upward warping of the pressure and pressure derivative curves. (2) The length of fractures mainly affects the early and middle stages of the well-testing curves. The longer the fractures, the smaller the value of the corresponding pressure and pressure derivative. The longer the fracture, the less noticeable the horizontal section of the pressure derivative curve in the fracture radial flow stage. (3) The distance between fractures mainly affects the mid-fracture radial flow stage and the formation linear flow stage. The closer the distance between fractures, the less noticeable the fracture radial flow stage, and it enters the formation linear flow stage earlier.

References

1. Wang, Z., Zhang, S., Wang, Y., Mou, S.: Research on productivity prediction of horizontal wells in low permeability gas reservoirs using different completion methods. J. Xi'an Petrol. Inst. (Nat. Sci. Ed.) **06**, 39–42 + 90–91 (2003)
2. Yao, J., Huang, C., Liu, W., Zhang, Y., Zeng, Q., Yan, X.: Key mechanical problems in deep oil and gas reservoir development. Chin. Sci. Phys. Mech. Astron. **48**(04), 5–31 (2018)
3. Terzaghi, K.: Theoretical Soil Mechanics. Wiley, New York (1943)
4. Biot, M.A.: General theory of three dimensional consolidation. Appl. Phys. **12**, 155–164 (1941)
5. Biot, M.A.: General solution of the equations of elasticity and consolidation for aporous material. J. Appl. Mech. **78**, 91–96 (1956)
6. Dong, P.: Fluid Solid Coupling Theory, Numerical Simulation and Application of Oil and Gas Reservoirs. Northeastern University, Shenyang (1998)
7. Ran, Q., Gu, X.: Numerical simulation of multiphase fluid flow in elastic-plastic deformation reservoirs. J. Comput. Mech. **16**(1), 24–31 (1999)
8. Zhou, Z.: Research on the Theory and Application of Fluid-Solid Coupling Seepage in Low Permeability Reservoirs. Daqing Petroleum Institute (2003)
9. Chin, L.Y., Raghavan, R., Thomas, L.K.: Full coupled geomechanics and fluid-flow analysis of wells with stress-dependent permeability. In: Proceedings of 1998 SPE International Oil and Gas Conference and Exhibition in China, 2–6 Nov 1998. Beijing, China. Soc. Petrol. Eng. J., 32–45 (1998)
10. Pinzon, C.L., Chen, H.Y., Teufel, L.W.: Numerical well test analysis of stress-sensitive reservoirs. In: Proceedings of 2001 SPE Rocky Mountain Petroleum Technology Conference, 21–23 May 2001. Keystone, Colorada, USA. Soc. Petrol. Eng. J. (2001)
11. Tao, O.F.: A Numerical Model of Fracture Permeability Change in Naturally Fractured Reservoirs Using a Fully Coupled Displacement Discontinuity Method. A&M University, Texas (2010)
12. Samaniego, V.F., Villalobos, L.H.: Transient pressure analysis of pressure-dependent naturally fractured reservoirs. J. Petrol. Sci. Eng. **39**(1/2), 45–56 (2003)
13. Pedrosa, O.A.: Pressure transient response in stress-sensitive formations. In: Proceedings of 1986 SPE California Regional Meeting, 2–4 Apr 1986. Oakland, California, USA. Soc. Petrol. Eng. J., 203–214 (1986)
14. Kikani, J., Pedrosa, O.A.: Perturbation analysis of stress-sensitive reservoirs. Soc. Pertrol. Eng. Format. Eval. **6**(3), 379–386 (1991)
15. Zhang, Z., He, S.: Characteristics of pressure recovery well testing curves in deformable media reservoirs. J. Chongq. Univ. **36**(11), 108–114 + 120 (2013)
16. Ran, Q., Li, S.: Research on the dynamic model of physical parameters in numerical simulation of fluid solid coupling oil reservoirs. Pet. Explor. Dev. **24**(3), 61–65 (1997)
17. Plastic Mechanics of Song Weidong. Science Press, Beijing (2017)
18. Zhuo, W.: Applied Elastoplastic Mechanics, pp. 23–25. Science Press, Beijing (2005)